Influence of the Temperature Gradient of the Two-phase Flow Mixture on the Pressure Drop Across the Bend

Lawan Abdullah Fahdil

Department of mechanical and mechatronic engineering, University of Salahaddin,Iraq/Erbil

lawanabdullahfadhillahmad@gmail.com

Iyd Eqqab Maree

Department of Aviation Engineering, University of Salahaddin,Iraq/Erbil

Iyd.maree@su.edu.krd

Abstract:

The current work presents an experimental demonstration of the impact of two-phase flow mixture (water and air) temperature on the pressure across the bend's upstream and downstream sides as well as the bend itself, as it is crucial for understanding and optimizing industrial processes. The test section in this study comprises a horizontal section, a vertical section, and a bend section, all made of PVC-U material with an inner diameter of 68 mm. The bend section has a curvature radius to diameter ratio (R/D) of 8. Pressure was monitored using six sensors over the test length for a range of water flow rates 18 to 42 m³/h and air flow rates 4 to 18 m³/h at various mixture temperatures. The obtained experimental pressure drop results were also compared to already previously published models to evaluate their performance in predicting pressure drop in conditions with heat transfer but no boiling. Based on the experimental result, the pressure across the test section increases with increasing temperature in a situation in which mixture viscosity is not dominated by liquid viscosity due to its high volume flow rate. Also, the pressure drop across the bend is higher at a lower air flow rate compared to a higher air flow rate at the same water flow rate and mixture temperature at room temperature, but as the mixture temperature increases, the pressure drop at a high air flow rate will be higher compared to a low air flow rate.

Keywords: Pressure drop, Two-phase flow, 90-degree elbow, Effect of Temperature

Nomenclature:

A	Area (m^2)	μ	Dynamic viscosity ($kg/(m \times s)$)
α	Void fraction	Φ	Two-phase pressure drop multiplier
C	heat capacity (J/(kg·K))	θ	Angle with respect to the horizontal
c_p	Specific heat capacity (kJ/kg. °C)	PLC	Programmable logic controller
d_i	Internal diameter (m)	Q	heat transfer (kJ)
ε	Surface roughness (m)	R	curvature radius (m)
Fr	Froude number	R_e	Reynolds number
g	Gravity (m/s^2)	Δp	Friction Pressure drop (pa)
G	Mass velocity ($kg/(m^2 \times s)$)	ρ	Density (kg / m^3)
H	Vertical height (m)	C_f	Darcy friction factors
j	Superficial velocity (m/s)	ΔL	Length of test section (m)
m	Mass flow rate (kg/s)	We	Weber number

Subscripts:

	g:gas	t:two-phase
L: liquid	h: horizontal,	v: vertical
H: homogenous	go: gas only	Lo: liquid only

1. Introduction:

The term "two-phase flow" refers to the interaction flow of two different phases in a channel, each representing a mass or volume of matter. Solid, gaseous, and liquid phases can all be found in the two phases. Since it is faced in many manufacturing applications, multiphase flow has become a key concern. The flow observed in the upstream petroleum industry is an excellent example of these processes. Beside its occurrence in nature, the two-phase flow has been studied by various researchers in order to enhance engineering applications such as heat exchangers [1], various heat radiators for electronic equipment [2], and two-phase solar heater [3]. Since two-phase flow offers a higher heat transfer capability and a more uniform temperature over the heat transfer surface than single-phase flow, it is one of the most promising cooling methods [4]. In industry, two-phase systems are common, but single-component systems are more common. The fundamental difference between two-phase single-component and two-phase two-component systems is that, when boiling is usually the main mechanism in the first, this is not the situation in the second. The two-phase two-component system is appealing because it can imitate the scenario of a two-phase single-component system while allowing for independent control of the gas-phase rate and attributes, which could be used further to enhance heat transfer in equipment [5].

There have been numerous studies on two-flow investigating the effect of various shapes, orientations of the geometry, and flow rates on two-phase flow pressure drop since the assessment of pressure drop in the system is one of the most common criteria for the design and sizing of industrial processes and equipment [6-8]. Industrial flow applications frequently

involve curved ducts with bends, such as U-type heat exchangers, steam boilers, transport pipelines, etc. For engineering design purposes, it is required to evaluate the pressure loss in fluid dynamic subcritical single-phase as well as two-phase flow. Authors in [7] experimentally studied the effect of superficial velocities of air and water on frictional pressure in straight pipes at different orientations and stated that as superficial velocities of air and water increased, the pressure drop increased. The authors [9] conducted a study on the behavior of air-water two-phase flows in PVC elbows with different diameters and curvature radius to diameter ratios using computational, experimental, and empirical methods. The study focused on the impact of significant parameters such as mass quality, mass flux, and curvature radius on the flow behavior. The results showed a substantial loss in energy and pressure as the fluid exits the elbow section, and a higher drop in pressure was observed at higher air velocity. Therefore, the study highlights the importance of understanding the behavior of two-phase flows in bends for designing efficient piping systems. Authors in [10] investigated the frictional pressure drop of air-water flow in wavy pipes with various diameters, curvature radii, and spacer lengths. The experimental results reveal that as the curvature ratio decreases, the two-phase pressure drop rises. Besides studying the factors that affect the pressure drop, researchers also studied the flow pattern, which is also one of the factors that influence the pressure drop [11-14].

Flow pattern maps, which are commonly depicted as two-dimensional graphs with multiple inside boundaries, are used to anticipate flow regimes and are usually based on a variety of data from experiment [15]. The authors [16]investigated the pressure drop and flow patterns of oil-water flows in a U-bend pipe. The results indicated that while the bend had limited influence on downstream flow patterns, it did cause a shift in flow pattern transition and bubble characteristics in the redeveloping flow section after the bend. The pressure gradient increased with both oil fraction and water superficial velocity, with a sharp change in pressure gradient profile during phase inversion. Pressure losses were strongly linked to the superficial velocity of the phases and the flow pattern, with higher pressure losses at the redeveloping section after the bend at high mixture velocities and at the bend in the straight sections at low mixture velocities. However, pressure drop generally decreased with the level of flow development downstream of the bend. These findings emphasize the importance of understanding the impact of flow pattern on pressure drop in designing and optimizing pipelines and other fluid transport system.Many researchers have related or described their heat transfer data in terms of different flow regimes, indicating that they have an effect on heat transfer in addition to pressure flow pattern [17].

Studying the pressure drop across the bend is more complicated than studying the pressure in a cross-strait pipe. Since the bends are curved in nature, the fluids entering the bend create centrifugal and viscous forces [18]. Also, the flow patterns developed are more complex than those of straight pipes since fluid motion in a bend is not parallel to the curved axis of the bend. As fluid flows through a curved pipe, the centrifugal force that acts at right angles to the main flow causes the denser phase (i.e., liquid) to move away from the center of curvature while the less dense face (i.e., air) flows toward the center of curvature [19]. Researchers found that when a two-phase flow passes over a bend, there is considerable vibration as a result of the two-phase flow's instability in terms of density, pressure, velocity, and momentum [20].

According to the researchers [21, 22], a two-phase flow could be used to enhance heat transfer, which could be used to enhance the performance of heat exchangers and solar collectors, which also contain bends. However, most available two-phase flow studies are focused on improving heat transfer, with few researchers focusing on the effect of two-phase flow temperature on the pressure drop, particularly across bends There is also research available on the pressure drops of two-phase flow that is either adiabatic or boiling, in which the temperature does not change. Since two-phase flow (water-air) is used to improve heat transfer, it includes a temperature gradient in two-phase flow that affects pressure drop, but there isn't enough research on the effect of temperature on pressure drop of two-phase flow in bends, which are widely used in many engineering applications. Therefore, this study aim is to evaluate experimentally the impact of the temperature gradient on the two-phase flow pressure drop in 90-degree elbows.

2. Experimental setup and tools:

Horizontal and vertical straight pipes with 90-degree bends were used experiment, in which they were composed of PVC-U material with an inner diameter of 68 mm and a bend with a curvature radius to diameter ratio (R/D) of 8, as shown in Fig (1). Water was stored in a tank with a volume of 0.53 m^3, and its temperature was regulated by two heaters, each of which was rated at 6 kW, driven by a PLC (programmable logic controller), with the help of temperature sensors inside the tank. The two-phase flow was made by mixing the water and the air in the mixer to accommodate the formation of a two-phase flow in the horizontal pipe. Water entered the mixer perpendicularly to its axis, and the air entered the mixer parallel to its axis through a pipe with drilled holes each 0.3 mm in diameter. The air-water mixture left the mixer from the opposite side of the air entrance. The schematic diagram of the air-water mixer can be seen in Fig (2). Water was supplied by a water pump with a flow rate range of 18 to 42 m^3/h; the air was supplied by an air compressor, and the flow rate was regulated to get the required flow rate up to 24 m^3/h. The water and the airflow rate were measured using a rotameter ranging between 6 to 42 m^3/h for water with accuracy of ±2% and 4-40 m^3/h for the air with accuracy of ±3%. Six pressure transmitters are used to measure the pressure across the two bends and straight (horizontal and vertical) sections of the pipe. The distance between each pressure sensor in the straight (horizontal and vertical) sections is one meter apart. For the two bends, one pressure transmitter is installed at the inlet and another at the outlet for each bend. The pressure transmitter used in this experiment is the Trafag (ECT4.0A) type, which can measure pressure between ranges of 0-4 bars with an accuracy of 0.5%FS (±0.02 bar) at 25 °C and can withstand medium temperatures up to 125 °C. The location of each transmitter and their spacing can be seen in Fig (3). The temperature sensors that were used in this experiment to measure the temperature of the water and mixture inside the tank and pipe were made of two different types. The temperature sensor (DS18B20) was used inside the tank due to its high accuracy (1%), and a K-Type Thermocouple with a MAX6675 Amplifier was used to measure the temperature inside the pipe due to its higher sampling rate compared to the DS18B20 because the mixture inside the pipe flows and K-Type Thermocouple with a MAX6675 Amplifier has accuracy of ±3%.

ARTICLE

The experimental producer for taking data is as follows:

1- The tank was filled with pure water and heated to the needed temperature (25 °C up to 70 °C) by using two heater roads, with their duty cycle (on, off) controlled by a PLC and feedback from a temperature sensor.

2- The motor and the compressor were turned on at the same time, water flowed inside the pipe while the air did not. It is stored in the tank compressor. The flow rate of water inside the pipe is adjusted to the desired flow by reading the rotameter and varying the voltage across the motor of the pump. Once water flow is steady, the valve for controlling the air flow rate is opened, and the desired air flow rate is set by reading the rotameter. The recording of data is started after stabilizing both flow rates at the required volume flow rate.

3- A computer application called ATmegacontroller retrieves pressure and temperature values from the PLC for a period of 30 seconds and plots them in an Excel sheet to initiate data collection. The air and water flow rates are then adjusted while keeping the water temperature constant.
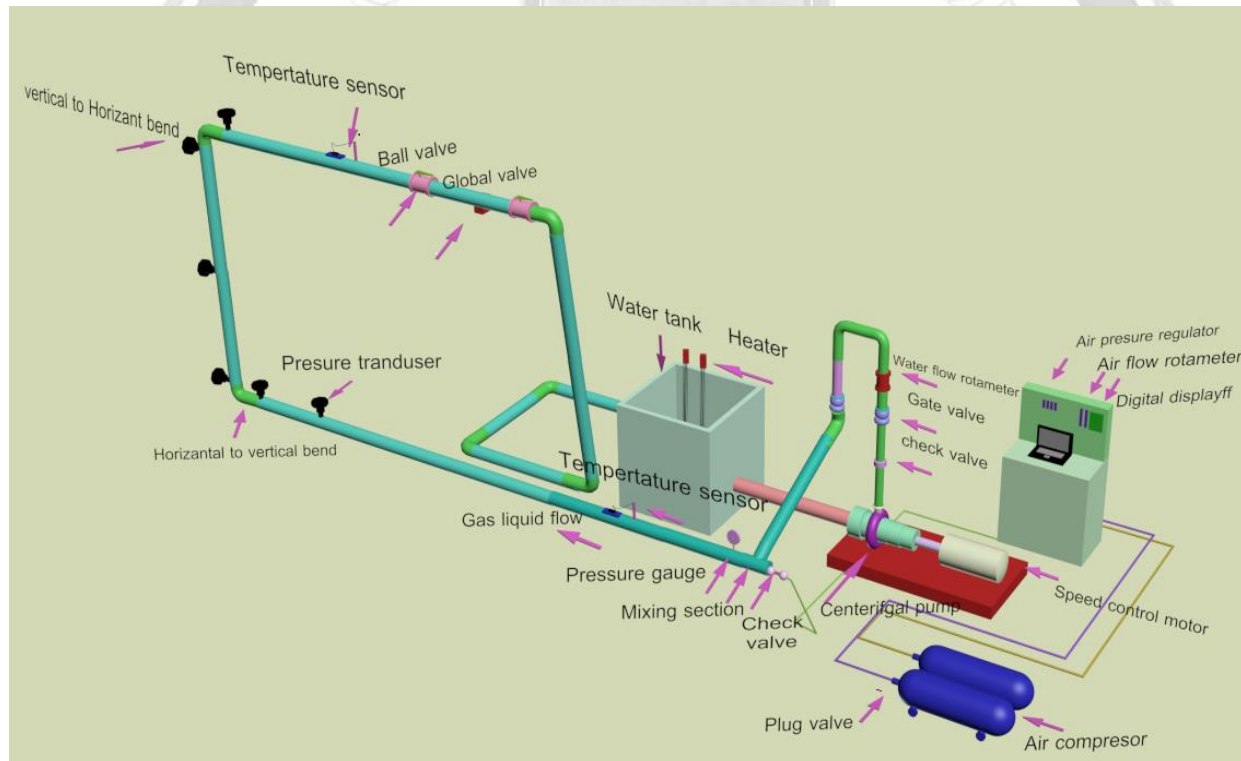

Fig.1: Diagram of the test section and the apparatus

Fig.2: Schematic diagram of the air-water mixer

Fig.3: The location of each transmitter and their spacing

3. Two-Phase Flow Pressure Drop Prediction Model:

Total pressure drop for two-phase flow in pipes consists of frictional, momentum, and gravitational components, where fractional pressure drop is due to friction at the pipe wall and liquid-gas interface and gravitational pressure drop is the pressure gradient due to gravity as a result of pipe elevation. The pressure difference caused by the expansion or contraction of the gas phase as the mixture of the two phases moves through the test section is called the acceleration pressure drops [7].The gravitational and acceleration pressure drops could be calculated as follows, respectively:

$$\Delta p_{grav} = \rho_m g H \sin\theta \qquad (1)$$

Where the mixture density (ρ_m) can be calculated by:

$$\rho_m = \alpha \rho_g + (1-\alpha)\rho_f \qquad (2)$$

Using the equations in Table 1, the void fraction for the horizontal and vertical sections could be calculated.

$$\Delta p_{acc} = \frac{G_t^2}{\Delta L}\left(\left(\frac{(1-x)^2}{\rho_L(1-\alpha)} + \frac{(x)^2}{\rho_g(\alpha)}\right)_o - \left(\frac{(1-x)^2}{\rho_L(1-\alpha)} + \frac{(x)^2}{\rho_g(\alpha)}\right)_i\right) \quad (3)$$

Prior research ignored the acceleration pressure drop for non-boiling two-phase flows in straight pipes, such as air-water two-phase flows, because it contributed so little to the overall pressure gradient; however, for two-phase flow in bends, the pressure loss is increased due to dissipation caused by momentum exchange between the phases and separation and remixing of the gas and liquid phases [7, 23]. The pressure gradient due to friction in two-phase flows is the most complex and difficult one to predict due to its dependency on pipe inclination, flow regime, and pipe roughness. The two most widely used methods for predicting frictional pressure drops are the homogenous model and the separated model. The homogeneous technique has a slip ratio of 1, meaning that the phases move at the same speed. As a result, the homogeneous model is sometimes referred to as the zero slip model. A two-phase flow is viewed by the homogeneous model as a single-phase flow with average fluid parameters that rely on mass quality. By supposing a constant friction coefficient between the pipe's intake and outlet sections, it is possible to determine the frictional pressure drop. The separated flow model accounts for the velocity difference between the gas and liquid phases in calculating the two-phase frictional pressure drop. Thus, the separated model is often referred to as the slip flow model. The separated model was built on the conventional work of Martinelli and Nelson and Lockhart and Martinelli [24]. The Lockhart-Martinelli method is one of the simplest methods for calculating two-phase frictional pressure drop and hold-up. One of the key advantages of the Lockhart-Martinelli technique is that it may be used with any flow pattern. This flexibility must be given up, though, for comparatively low precision. In a separate modeling technique, there are four ways to define the two-phase frictional pressure gradient in terms of the two-phase multiplier that takes into consideration the frictional pressure gradient of single-phase flows [7, 24].

$$\Delta P_t = \Phi_L{}^2 \Delta P_L \quad (4)$$

$$\Delta P_t = \Phi_g{}^2 \Delta P_g \quad (5)$$

$$\Delta P_t = \Phi_{Lo}{}^2 \Delta P_{Lo} \quad (6)$$

$$\Delta P_t = \Phi_{go}{}^2 \Delta P_{go} \quad (7)$$

The subscripts L and g are used for frictional pressure drop when the single-phase liquid or gas is flowing at a mass flux of $G_L = (G_t(1-x))$ and $G_g = (G_t(x))$, but Lo and go are used when the single-phase liquid or gas flow rate is assumed to be equivalent to the two-phase flow mixture mass flux G_t. In this study, for the horizontal section, only the friction pressure drop is taken into account; however, for the vertical section, both the friction pressure drop and the change in static head are taken into account. The used models for predicting pressure drop across the straight pipe are tabulated in Table 2. Also, for the bend, there are three models used to predict pressure drops, which are tabulated in Table 3. The suggested models in Tables 2 and 3

are based on the two-phase flow property, which depends on temperature and pressure in some cases. However, heat transfer is not considered in these models because they were created for adiabatic or phase-change processes, in which the temperature does not change. In this study, the properties of air and water are evaluated at a temperature that is determined under the assumption of no heat loss to the environment. All heat lost by the liquid is gained by the air, and both fluids uniformly attain the same temperature. This assumption can be made due to the use of PVC-U material for the pipe, which has low thermal conductivity (0.14 W/m.K) at room temperature and is therefore a poor conductor of heat. Additionally, the minimum heat capacity rate affects the maximum heat transfer rate. The temperature was calculated using the equations given below, which are based on [25].

$$Q_{max} = C_{min}(T_{Li} - T_{gi}) \tag{8}$$

$$C_L = c_{p\,L}m_L \tag{9}$$

$$C_g = Cp_g m_g \tag{10}$$

$$C_{min} = smallest\ C_g, C_L \tag{11}$$

$$T_{Lo} = T_{Li} - \frac{Q_{max}}{C_L} \tag{12}$$

$$T_{go} = T_{gi} + \frac{Q_{max}}{C_g} \tag{13}$$

4. Results and Discussion

4.1. Effect of temperature on pressure in the two-phase flow:

The plots in Fig (4) depict the pressure of the two-phase flow as a function of time for six pressure transmitters at various test section locations, with a constant volume flow rate of water ($36\,\mathrm{m^3/h}$) and air ($12\,\mathrm{m^3/h}$) for a duration of about 30 s. Each plot corresponds to a different temperature. Based on Fig (4), it is observed that the pressure at each point of the sensor location fluctuates with time but increases with increasing temperature, and the same phenomena was also observed by [26]. The average pressure reading over 30 seconds for each of the six pressure transducers is plotted against temperature in Fig 5 and 6 for two different water flow rates of $36\,\mathrm{m^3/h}$ and 24 $\mathrm{m^3/h}$, respectively, to further demonstrate how temperature influences pressure. This demonstrates that the pressure increases as the temperature increases, with the exception of the low air flow rate at the high water flow rate, where the pressure actually decreases as the temperature increases due to a decrease in the mixture's viscosity, which is influenced by water's viscosity due to its high volume flow rate relative to air's flow rate. As reported by researcher [27] in his paper, the experiment revealed that the two-phase flow pressure gradient is highly dependent on liquid viscosity, with higher viscosity resulting in an increase in the pressure gradient. Fig (7) presents two plots of the pressures obtained from six pressure sensors as a function of temperature for the scenario where only water flows inside the pipe. The plots demonstrate that as the temperature increases, the pressure decreases due to the

viscosity at both flow rates. However, when air is mixed with the water, the low water flow rate`s viscosity does not have as much of an impact on the mixture`s viscosity as it does with the high water volume flow rate.

Fig.4A.   Instantaneous pressure at Mixture temperature (30 °C) for flow rate of Water

(36 m³/h) And air (12 m³/h)

Fig.4B.   Instantaneous pressure at Mixture temperature (70 °C) for flow rate of Water
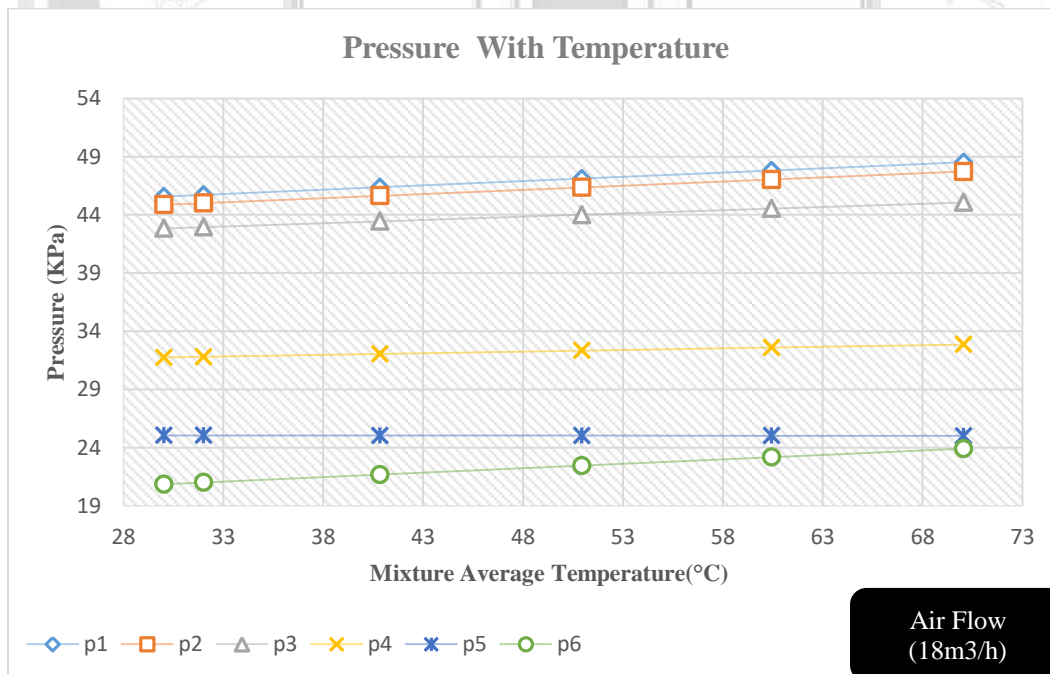
(36 m³/h) And air (12 m³/h)
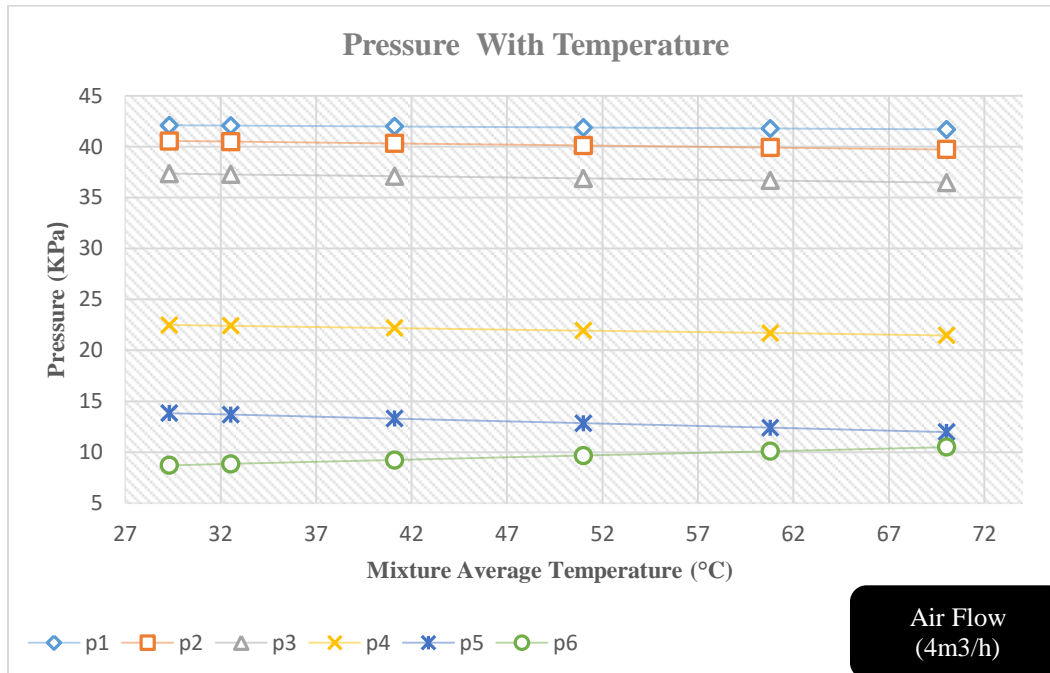
Fig.5A. Instantaneous pressure as function of temperature at air flow (4m^3/h) rate for (36m^3/h) Water flow rate
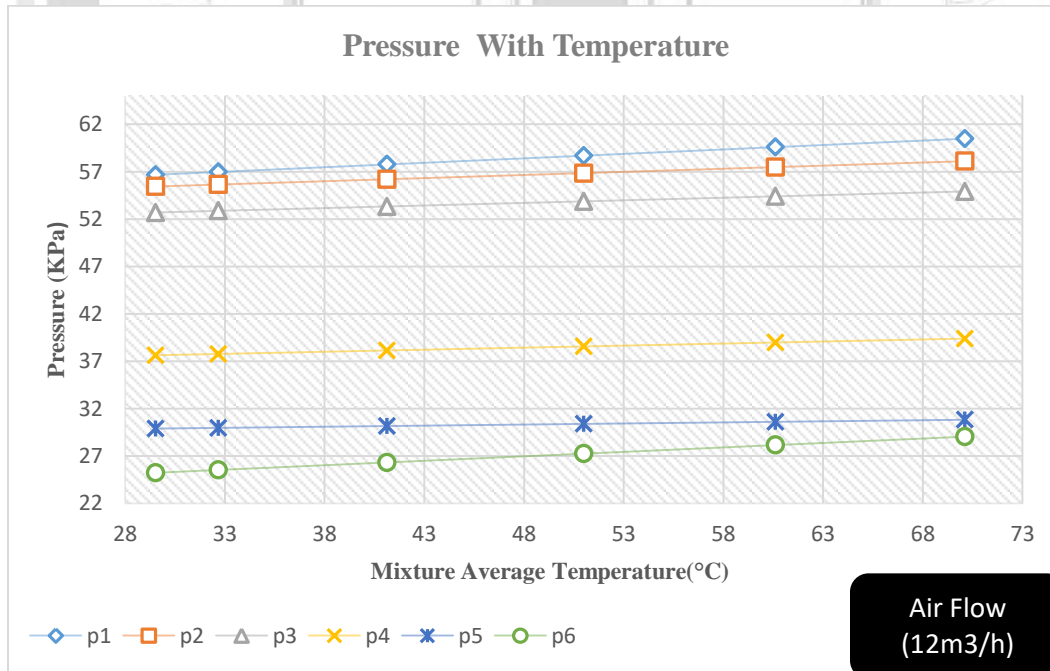
Fig.5B. Instantaneous pressure as function of temperature at air flow (12m^3/h) rate for (36m^3/h) Water flow rate
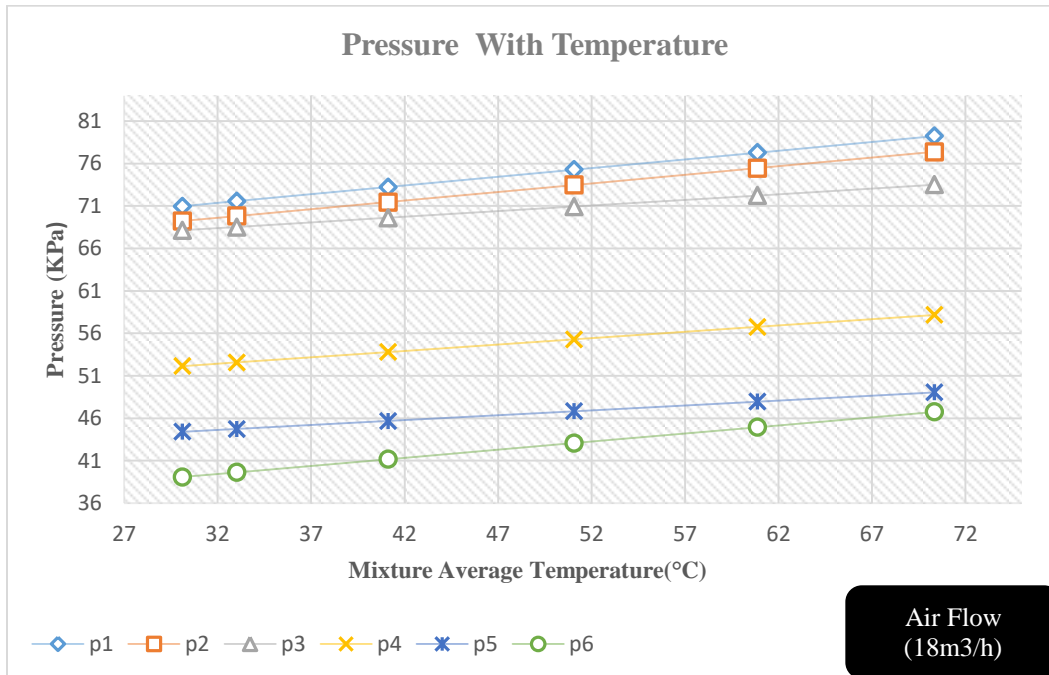
Fig.5C. Instantaneous pressure as function of temperature at air flow (18m^3/h) rate for (36m^3/h) Water flow rate
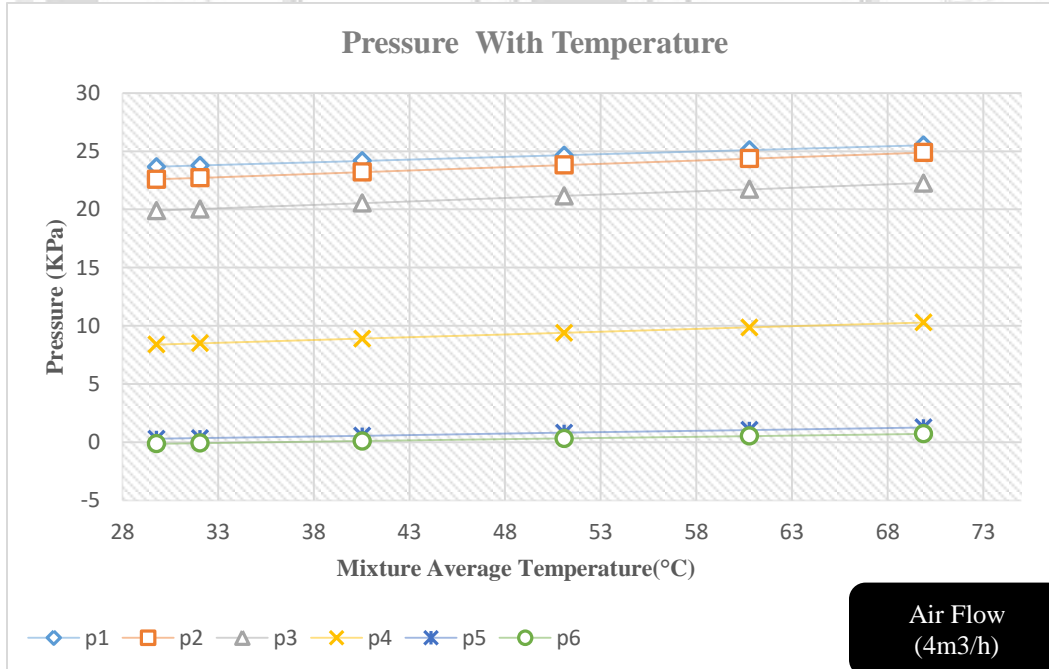
Fig.6A. Instantaneous pressure as function of temperature at air flow rate (4 m^3/h) for (24 m^3/h) Water flow rate

ARTICLE
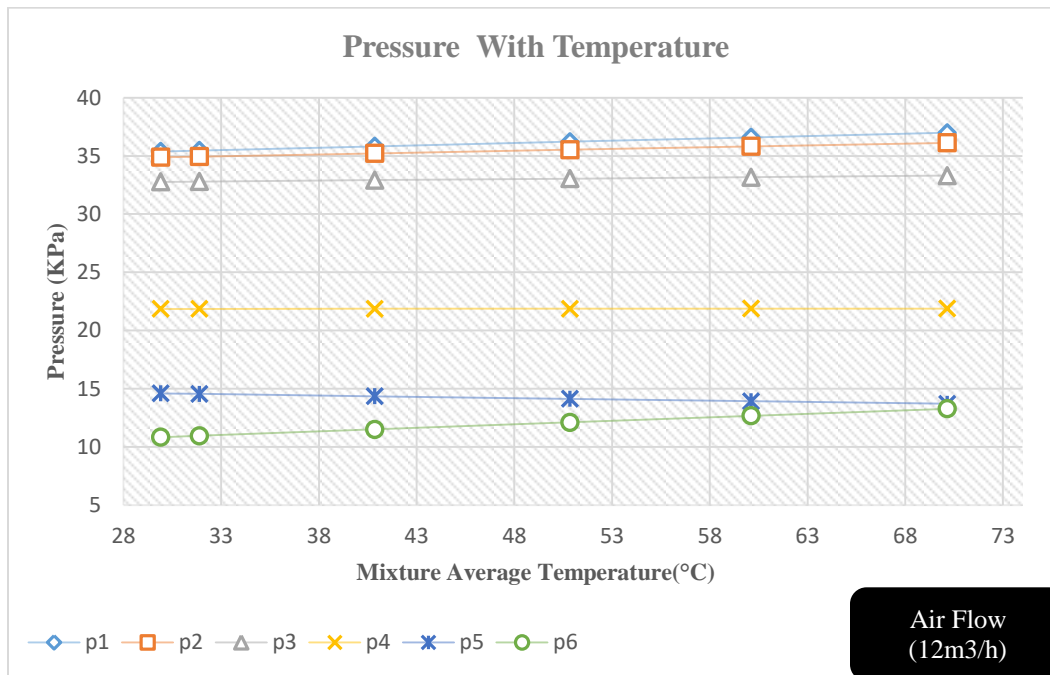
Fig.6B. Instantaneous pressure as function of temperature at air flow rate (12 m^3/h)

for (24 m^3/h) Water flow rate

Fig.6C. Instantaneous pressure as function of temperature at air flow rate (18 m^3/h)

for (24 m^3/h) Water flow rate
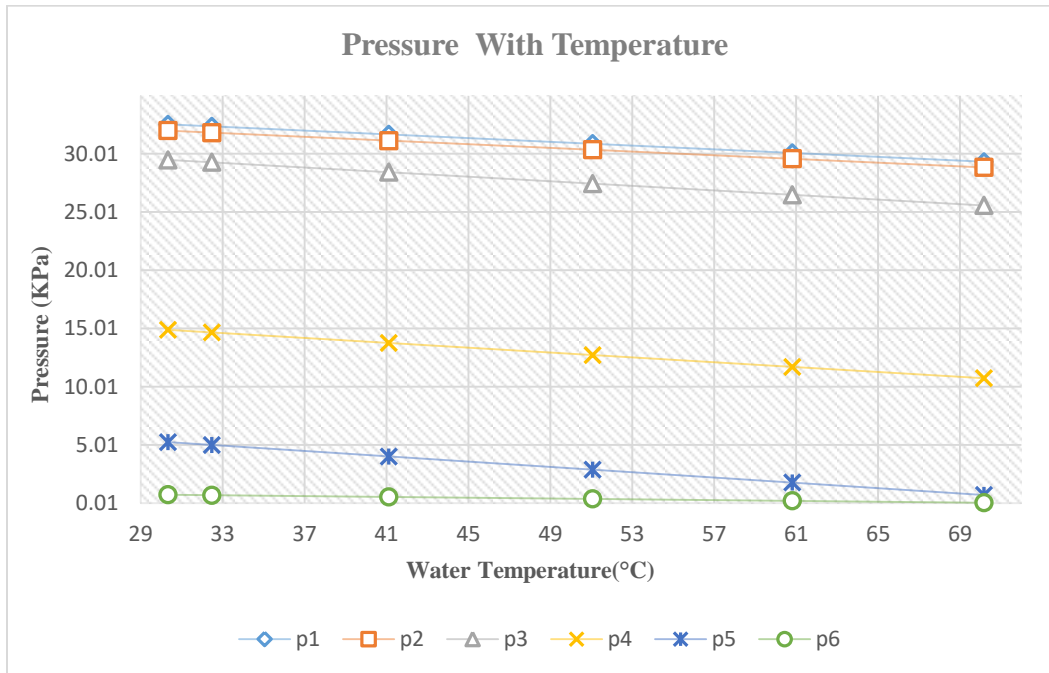
Fig.7A. Instantaneous pressure as function of temperature for water flow rate (36 m³/h)
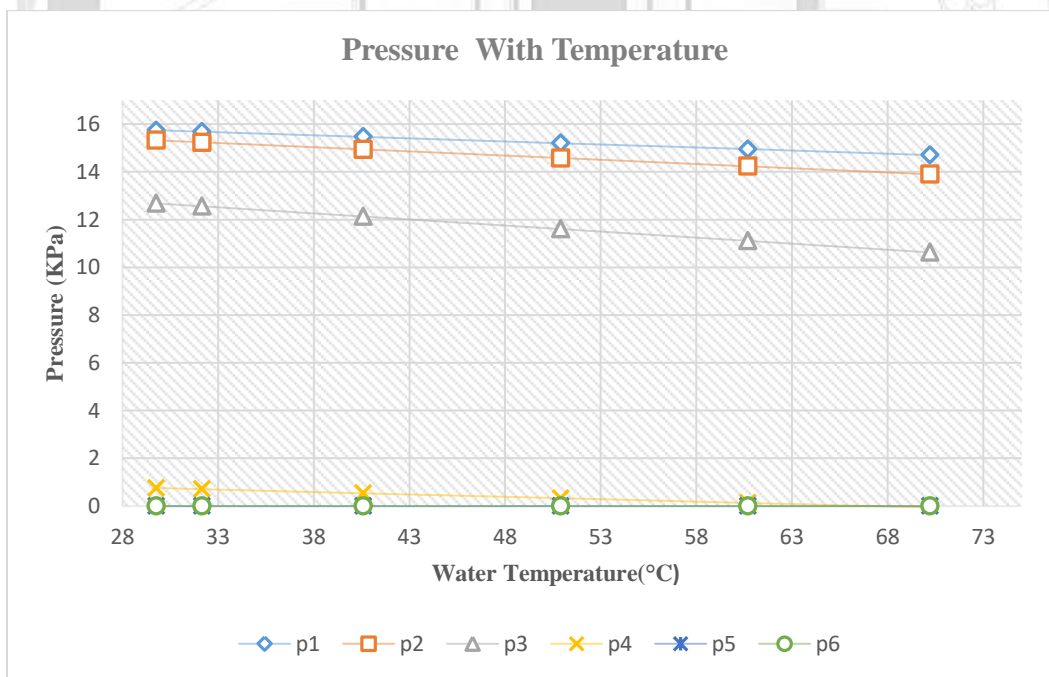
Fig.7B. Instantaneous pressure as function of temperature for water flow rate (24 m³/h)

4.2 Effect of temperature on pressure drop across the bend:

The pressure data collected from six test points is converted into differences that relate to different parts of the pipe: (p1-p2) for the horizontal segment, (p2-p3) for the first bend, (p3-p4 and p4-p5) for the vertical segment, and (p5-p6) for the second bend. This research primarily examined the pressure drop of the first bend, which is horizontal to vertical, due to the impact of the first bend on the second bend, which is vertical to horizontal. The second bend data was collected but will not be discussed in this work. This effect was also indicated by a researcher [28], who found that the impact of the elbow increases as it moves further downstream from the elbow. Four plots are shown in Figure 8, each representing a different water flow rate and each depicting the pressure drop around the bend for varied air flow with temperature. The pressure drop over the bend at room temperature is greater for low air flow rates compared to high air flow rates, according to the graphs in Figure 8 based on experimental results. High water flow rates cause bubble formation, which in turn causes high pressure drops at low air flow rates. According to [29] research, when high water flow rates and low air flow rates cross the bend, the bend acts as a droplet generator. However, at high air flow rates, the denser phase—that is, the liquid—moves away from the centre of curvature due to the centrifugal force produced by the curvature, while the air flows in the opposite direction, and this type of phase separation is likely to result in a lower pressure drop [19]. The authors in [30] claim that the viscosity of the fluid along the pipe wall causes it to travel more slowly than the fluid in the middle, necessitating a smaller pressure gradient to make up for the diminished centrifugal force. As the temperature of water rises, the pressure drop across the bend increases due to heat transfer between air and water, which causes the kinetic energy of the air molecules to increase and leads to higher air velocities and a greater void fraction. This is consistent with the findings of researchers[31], who found that an increase in superficial gas velocity leads to a higher void fraction, and the observations made by researchers [32] that at higher values of superficial gas velocity and void fraction, the frictional pressure drop becomes more sensitive to these parameters. At the higher liquid superficial velocity, the pressure drop is also less sensitive to changes in void fraction compared to the lower liquid superficial velocity. According to the plots in Figure 8, for low air flow rates, high water flow rates (30 and 36 m^3/h) cause a lower pressure drop as the mixture's temperature rises, but low water flow rates (18 m^3/h) cause a bigger pressure drop as the mixture's temperature rises. The lower pressure drop at a high water flow rate and low air flow rate as temperature increases is due to a reduction in the mixture's viscosity, which is affected by water's viscosity because of its large volume flow rate in comparison to air's flow rate. The effect of mixture viscosity also starts to take effect at a certain water flow rate (24 m^3/h).

Fig.8A. pressure drop across the bend for a water flow rate of $(18 \text{ m}^3/\text{h})$ and various air flow rates at different temperatures.

Fig.8B. pressure drop across the bend for a water flow rate of $(24 \text{ m}^3/\text{h})$ and various air flow rates at different temperatures.
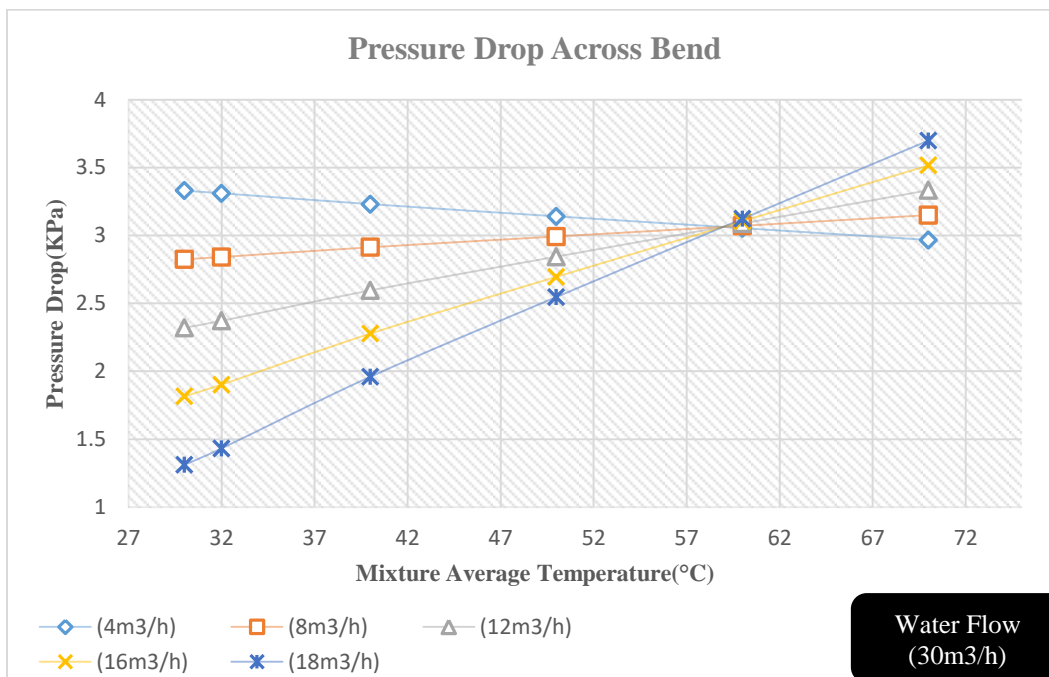
Fig.8C. pressure drop across the bend for a water flow rate of $(30\ \mathrm{m^3/h})$ and various air flow rates at different temperatures.
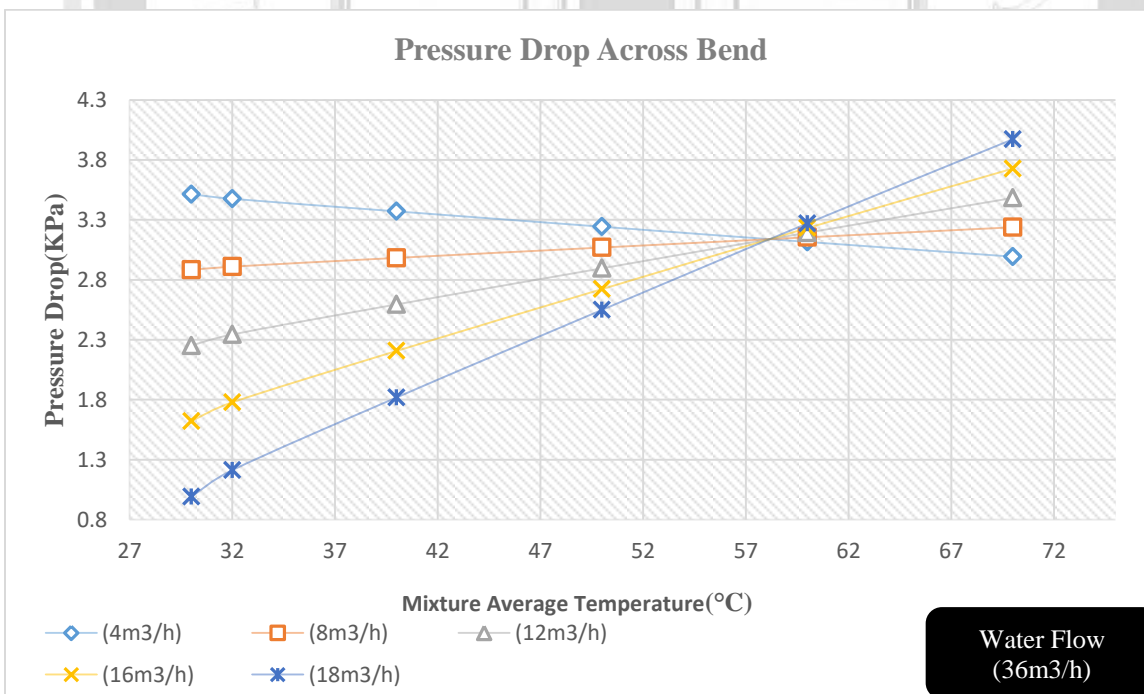
Fig.8D. pressure drop across the bend for a water flow rate of $(36\ \mathrm{m^3/h})$ and various air flow rates at different temperatures.

4.2 Compression between the pressure-predicting model and excremental data:

To compare the experimental and prediction model data in Tables 2 and 3, they were plotted separately for each region of the test section, as shown in Figures 9, 10, and 11, for bend, straight, and vertical, respectively. Based on Fig 9, it appears that the Chisolm B equation showed good agreement with the experimental result at a lower water flow rate and lower temptresses of the mixture, but for a higher water flow rate, the Aziz module showed good agreement with the experiment result at a lower temperature. For higher mixture temperatures and water flows, only the Chisolm B equation showed reasonable agreement. For the horizontal section of the pipe, the al model showed good agreement at low temperatures, but as the temperature increased, the difference between the experimental and prediction models increased. None of the models could accurately predict pressure in the vertical section of the pipe, as shown in Fig 11. The use of a correlation beyond the range of fluid parameters, test conditions, or pipe diameter from which the correlation was acquired is the primary cause of the discrepancy between the pressure perdition model and experiment data.
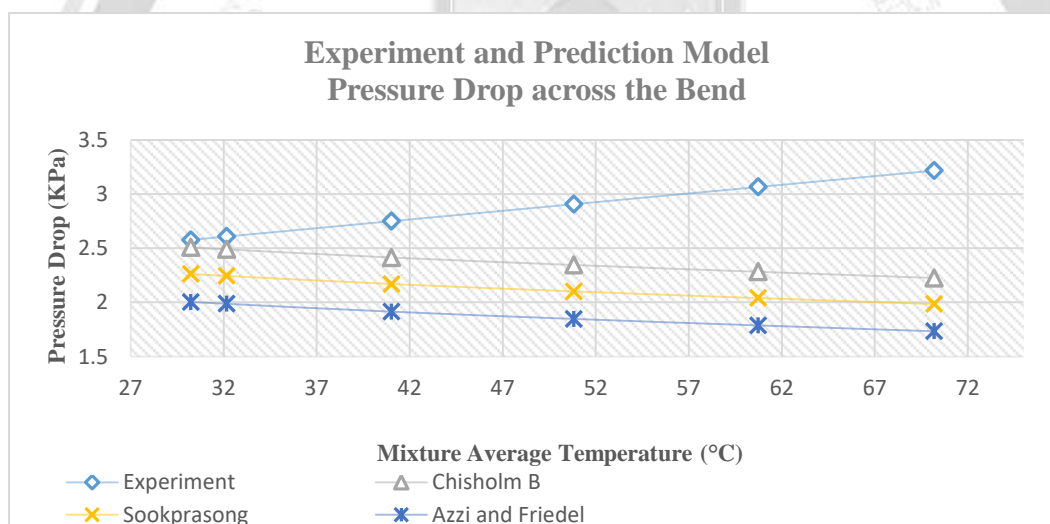

Fig.9A. Compression between the pressure-predicting model and experimental data across the bend for water (30 m^3/h) and air (12 m^3/h)
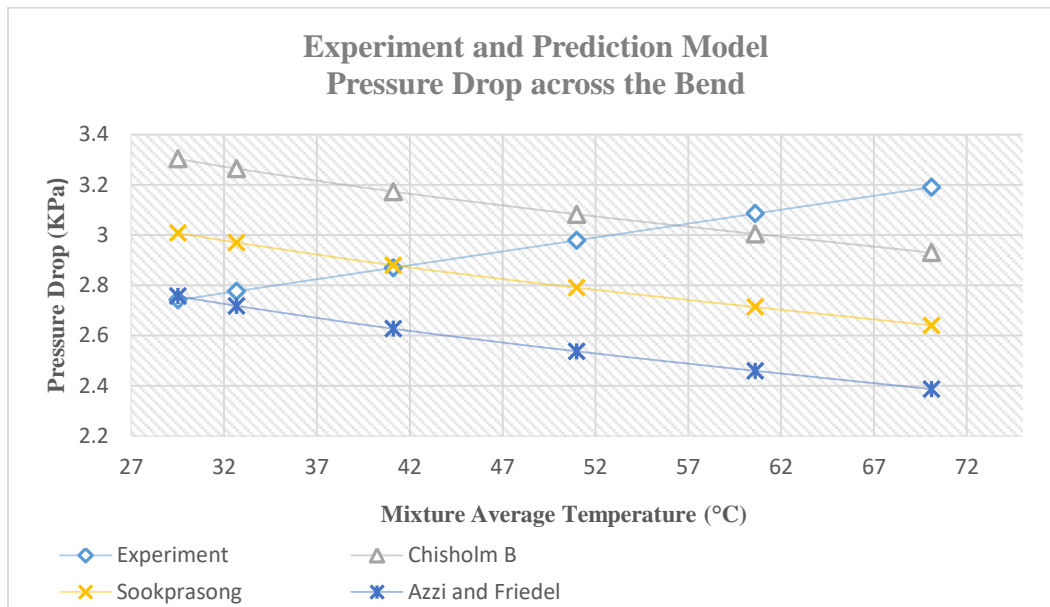
Fig.9B. Compression between the pressure-predicting model and experimental data across the bend for water (36 m^3/h) and air (12 m^3/h)

Fig. 10A. Compression between the pressure-predicting model and experimental data across the Horizontal section for water (30 m^3/h) and air (12 m^3/h)
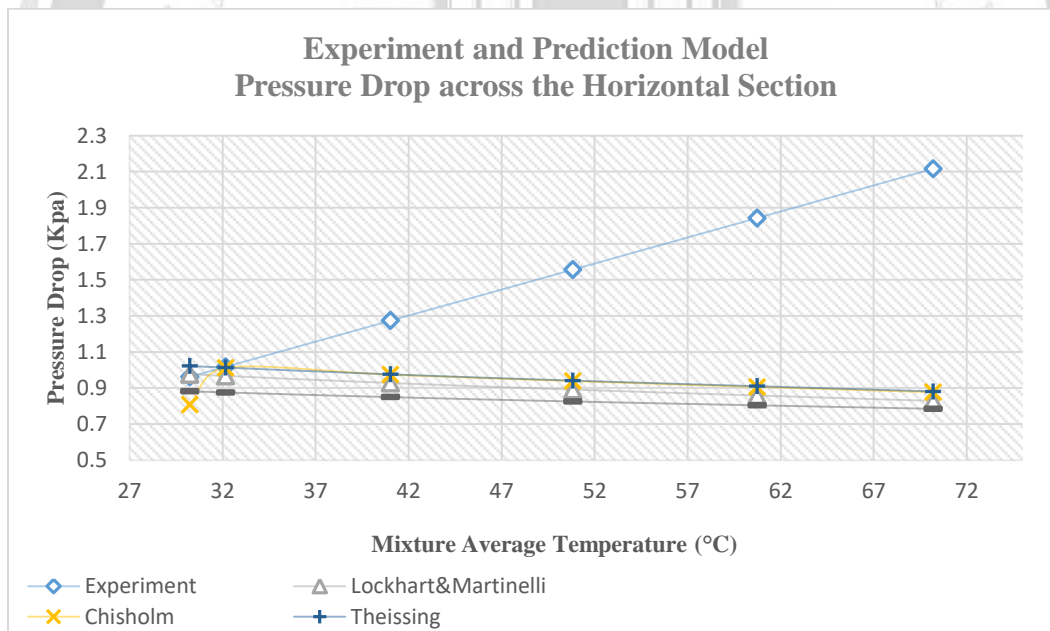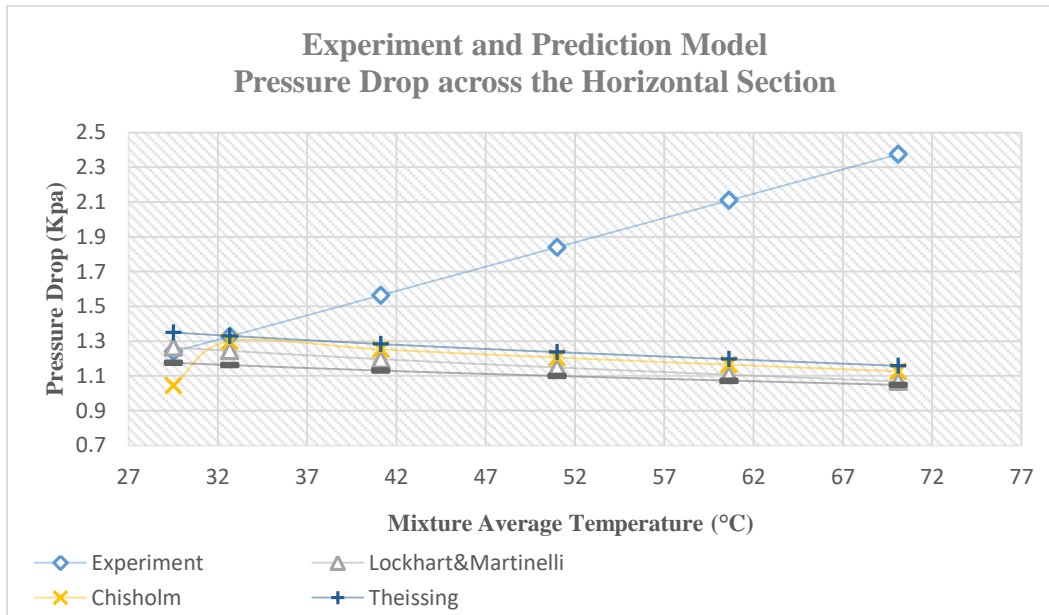
Fig. 10B. Compression between the pressure-predicting model and experimental data across the Horizontal section for water (36 m³/h) and air (12 m³/h)
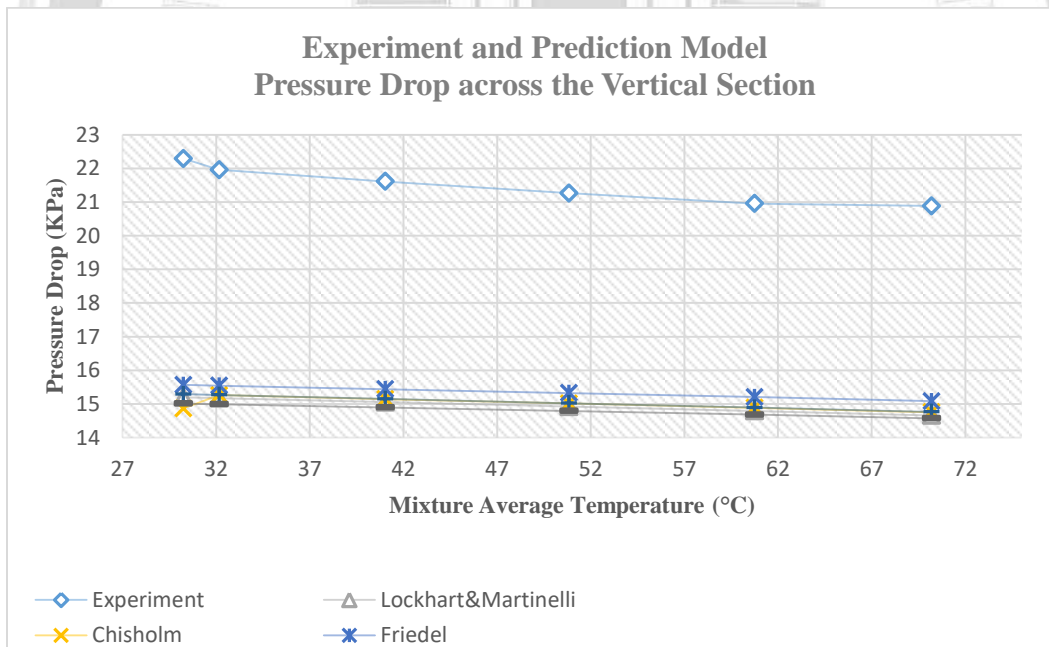

Fig. 11A. Compression between the pressure-predicting model and experimental data across the vertical section for water (30 m³/h) and air (12 m³/h)
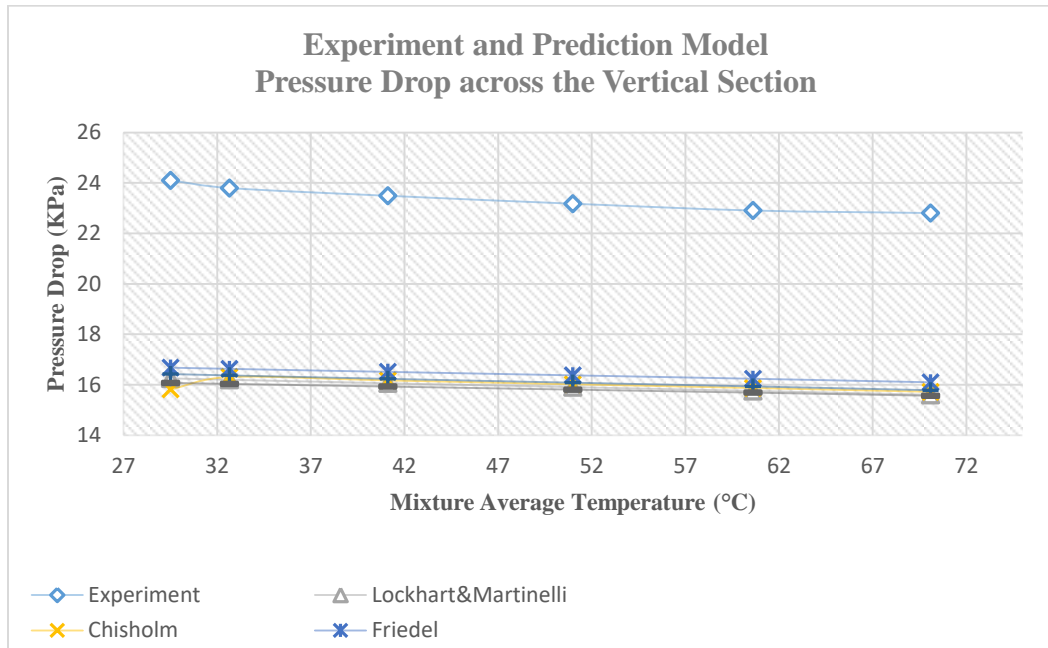
Fig. 11A. Compression between the pressure-predicting model and experimental data across the vertical section for water (36 m³/h) and air (12 m³/h)

5 Conclusions:

1- The results of the experiments showed that along the horizontal, vertical, and bending parts of the test section, the pressure went up as the temperature of the two-phase flow mixture went up. This was not the case for low airflow and high water flow, where the pressure went down because the viscosity of the mixture went down, which was caused by the high volume flow rate of the liquid.

2- Increasing the air volume flow rate at a lower temperature and maintaining the same water volume flow rate reduced the pressure drop around the bend. However, as the temperature rises, the pressure drop across the bend increases at the same water flow rate. The increased kinetic energy of air molecules as temperature rises causes the high-pressure drop.

3- At low air flow rates and lower temperatures, the formation of bubbles results in a high-pressure drop over the bend; but as the temperature increases, it leads to a greater pressure drop when the water level is low. However, as the water flow rose at the same airflow, it resulted in a smaller pressure drop.

4- For the bend and horizontal section, the pressure prediction model showed fair agreement with experimental data at low temperatures, but as the temperature rose, it did not, and for the vertical section, none of the pressure prediction approaches could accurately predict the pressure drop as a result of the "not in counting bend effect".

6 Reference

[1] P. Vlasogiannis, G. Karagiannis, P. Argyropoulos, and V. Bontozoglou, "Air–water two-phase flow and heat transfer in a plate heat exchanger," International Journal of Multiphase Flow, vol. 28, no. 5, pp. 757-772, 2002.

[2] G. Hetsroni, A. Mosyak, E. Pogrebnyak, and Z. Segal, "Heat transfer of gas–liquid mixture in micro-channel heat sink," International Journal of Heat and Mass Transfer, vol. 52, no. 17-18, pp. 3963-3971, 2009.

[3] V. Panthalookaran and J. P. George, "Experimental Study on Cooling of Solar Collectors Using Air-water Mixture," Energy Procedia, vol. 91, pp. 303-311, 2016, doi: 10.1016/j.egypro.2016.06.222.

[4] B. Agostini, M. Fabbri, J. E. Park, L. Wojtan, J. R. Thome, and B. Michel, "State of the art of high heat flux cooling technologies," Heat Transfer Engineering, vol. 28, no. 4, pp. 258-281, 2007.

[5] M. I. Alahmad, "Analysis of Heat Transfer in Two-Phase Two-Component Mixtures," Journal of King Saud University - Engineering Sciences, vol. 5, no. 2, pp. 257-289, 1993, doi: 10.1016/s1018-3639(18)30584-1.

[6] A. J. Ghajar and S. M. Bhagwat, "Flow patterns, void fraction and pressure drop in gas-liquid two phase flow at different pipe orientations," in Frontiers and progress in multiphase flow I: Springer, 2014, pp. 157-212.

[7] C. Lu et al., "Frictional pressure drop analysis for horizontal and vertical air-water two-phase flows in different pipe sizes," Nuclear Engineering and Design, vol. 332, pp. 147-161, 2018, doi: 10.1016/j.nucengdes.2018.03.036.

[8] S. S. Ibrahim and L. A. Abdulkareem, "Pressure Drop in Horizontal Two-Phase Flow," Engineering, Technology & Applied Science Research, vol. 12, no. 4, pp. 9063-9070, 2022.

[9] H. A. Saber and I. E. Maree, "A computational study of curvature effect on pressure drop of gas-liquid two-phase flow through 90 degree elbow," Thermal Science, no. 00, pp. 2-2, 2022.

[10] I. Chen, J. Huang, and C.-C. Wang, "Single-phase and two-phase frictional characteristics of small U-type wavy tubes," International communications in heat and mass transfer, vol. 31, no. 3, pp. 303-314, 2004.

[11] G. Hetsroni, "Handbook of multiphase systems," 1982.

[12] J. G. Collier and J. R. Thome, Convective boiling and condensation. Clarendon Press, 1994.

[13] V. A. Musa, L. A. Abdulkareem, and O. M. Ali, "Experimental Study of the Two-Phase Flow Patterns of Air-Water Mixture at Vertical Bend Inlet and Outlet," Engineering, Technology & Applied Science Research, vol. 9, no. 5, pp. 4649-4653, 2019.

[14] L. A. Abdulkareem, "Identification of Oil-Gas Two Phase Flow in a Vertical Pipe using Advanced Measurement Techniques," Engineering, Technology & Applied Science Research, vol. 10, no. 5, pp. 6165-6171, 2020.

ARTICLE

[15] N. P. del Corral, "Analysis of Two-Phase Flow Pattern Maps," Brno University of Technology, 2014.

[16] P. O. Ayegba, L. C. Edomwonyi-Otu, A. Abubakar, and N. Yusuf, "Flow pattern and pressure drop for oil–water flows in and around 180° bends," SN Applied Sciences, vol. 3, pp. 1-13, 2021.

[17] Y. Gao et al., "Two phase flow heat transfer analysis at different flow patterns in the wellbore," Applied Thermal Engineering, vol. 117, pp. 544-552, 2017, doi: 10.1016/j.applthermaleng.2017.02.058.

[18] S. Debnath, A. Banik, T. K. Bandyopadhyay, and A. K. Saha, "CFD and optimization study of frictional pressure drop through bends," Recent Patents on Biotechnology, vol. 13, no. 1, pp. 74-86, 2019.

[19] S. N. Mandal and S. K. Das, "Pressure losses in bends during two-phase gas− Newtonian liquid flow," Industrial & engineering chemistry research, vol. 40, no. 10, pp. 2340-2351, 2001.

[20] U. Khan, W. Pao, and N. Sallih, "A Review: Factors Affecting Internal Two-Phase Flow-Induced Vibrations," Applied Sciences, vol. 12, no. 17, p. 8406, 2022.

[21] P. Suwankamnerd and S. Wongwises, "An experimental study of two-phase air–water flow and heat transfer characteristics of segmented flow in a microchannel," Experimental Thermal and Fluid Science, vol. 62, pp. 29-39, 2015.

[22] S. Saisorn, P. Kuaseng, and S. Wongwises, "Heat transfer characteristics of gas–liquid flow in horizontal rectangular micro-channels," Experimental thermal and fluid science, vol. 55, pp. 54-61, 2014.

[23] A. Azzi and L. Friedel, "Two-phase upward flow 90° bend pressure loss model," Forschung im Ingenieurwesen, vol. 69, no. 2, pp. 120-130, 2005/03/01 2005, doi: 10.1007/s10010-004-0147-6.

[24] M. M. Awad and Y. S. Muzychka, "A simple two-phase frictional multiplier calculation method," 2004, vol. 41766, pp. 475-483.

[25] Y. Cengel and T. M. Heat, "A practical approach," Second edi, 2003.

[26] I. M. Abed, "Performance Analysis, Pressure Drop and Phases-Distribution for Oil-Water-Air Three-Phase Flow Through Vertical Pipe," Journal of Engineering and Applied Sciences, vol. 14, no. 4, pp. 1365-1373, 2019.

[27] S. Sukamta and S. Sudarja, "The Significant Effect of Liquid Viscosity on Two-Phase Flow Pressure Gradient in Mini Channel with Slope of 15o against Horizontal," Journal of Advanced Research in Fluid Mechanics and Thermal Sciences, vol. 70, no. 2, pp. 116-123, 2020.

[28] S. Kim, J. H. Park, G. Kojasoy, and J. Kelly, "Two-phase frictional pressure loss in horizontal bubbly flow with 90-degree bend," 2006, vol. 42436, pp. 227-233.

[29] P. L. Spedding, E. Bénard, and G. M. McNally, "Two-and Three-Phase Flow Through a 90 Degree Bend," Developments in Chemical Engineering and Mineral Processing, vol. 13, no. 5-6, pp. 719-730, 2005.

[30] P. Dutta, S. K. Saha, and N. Nandi, "Numerical study of curvature effect on turbulent flow in 90 pipe bend," Dep. of Aerospace Eng. and Applied Mechanics, ICTACEM-2014/028, 2014.

[31] R. C. Bowden, É. Lessard, and S.-K. Yang, "Void fraction measurements of bubbly flow in a horizontal 90 bend using wire mesh sensors," International Journal of Multiphase Flow, vol. 99, pp. 30-47, 2018.

[32] C. C. Tang, S. Tiwari, and A. J. Ghajar, "Effect of void fraction on pressure drop in upward vertical two-phase gas-liquid pipe flow," Journal of engineering for gas turbines and power, vol. 135, no. 2, 2013.

[33] J. Thome, "Engineering Data Book III, Chapter 13, Two–phase pressure drops, Wolverine Tube," ed: Inc, 2004.

[34] D. Chisholm, "Pressure gradients due to friction during the flow of evaporating two-phase mixtures in smooth tubes and channels," International Journal of Heat and Mass Transfer, vol. 16, no. 2, pp. 347-358, 1973.

[35] L. Friedel, "Improved friction pressure drop correlation for horizontal and vertical two-phase pipe flow," Proc. of European Two-Phase Flow Group Meet., Ispra, Italy, 1979, 1979.

[36] H. Müller-Steinhagen and K. Heck, "A simple friction pressure drop correlation for two-phase flow in pipes," Chemical Engineering and Processing: Process Intensification, vol. 20, no. 6, pp. 297-308, 1986.

[37] B. A. Shannak, "Frictional pressure drop of gas liquid two-phase flow in pipes," Nuclear Engineering and Design, vol. 238, no. 12, pp. 3277-3284, 2008.

[38] P. Theissing, "Generally valid method for calculating frictional pressure drop on multiphase flow," Chem.-Ing.-Tech.;(Germany, Federal Republic of), vol. 52, no. 4, 1980.

[39] V. D. Chisholm, "Two-phase flow in bends," International Journal of Multiphase Flow, vol. 6, no. 4, pp. 363-367, 1980.

[40] P. Sookprasong, J. P. Brill, and Z. Schmidt, "Two-phase flow in piping components," 1986.

Appendix A:

Table 1: Void fraction equations

Author or methods	All required equations
Void fraction equation for horizontal pipe[33]	$$\alpha_h = \frac{x}{p_G}\left(\left(1 + 0.12(1-x)\right)\left(\frac{x}{P_G} + \frac{(1-x)}{P_L}\right)\right.$$ $$\left. + \frac{1.18(1-x)\left(g\sigma(p_L - p_G)\right)^{0.25}}{G_t p_L{}^2}\right)^{-1}$$
Void fraction equation for vertical pipe[33]	$$\alpha_v = \frac{x}{p_G}\left(\left(1 + 0.2(1-x)\left(\frac{gDP_L{}^2}{G_t{}^2}\right)^{\frac{1}{4}}\right)\left(\frac{x}{P_G} + \frac{(1-x)}{P_L}\right)\right.$$ $$\left. + \frac{1.18(1-x)\left(g\sigma(p_L - p_G)\right)^{0.25}}{G_t p_L{}^2}\right)^{-1}$$

Table 2: Two phase flow multiplier equations for horizontal and vertical section

Author or methods	All required equations
Homogenous method [33]	$$\Delta P_t = \frac{2C_{f_t}LG_t{}^2}{d_i\rho_H}, C_{f_t} = \frac{0.079}{R_e{}^{0.25}}, R_e = \frac{G_t d_i}{u_H}, u_H = xu_g + (1-x)u_L,$$ $$\rho_H = \alpha\rho_g + (1-\alpha)\rho_L, \alpha = \frac{1}{1 + \left(\left(\frac{u_g}{u_L}\right)\left(\frac{1-x}{x}\right)\left(\frac{\rho_g}{\rho_L}\right)\right)}, x = \frac{m_g}{m_g + m_L},$$ $$G_L = \frac{m_L}{A}, G_g = \frac{m_g}{A}, G_t = G_l + G_g$$
Lockhart and Martinelli [33]	$$\Delta P_L = \Phi_L{}^2\Delta P_L,, \Delta P_g = \Phi_g{}^2\Delta P_g, \Delta P_L = 4C_{f_L}\left(\frac{\Delta L}{d_i}\right)G_t{}^2(1-x)^2\left(\frac{1}{2\rho_L}\right),$$ $$\Delta P_g = 4C_{f_g}\left(\frac{\Delta L}{d_i}\right)G_t{}^2(x)^2\left(\frac{1}{2\rho_g}\right), C_{f_L} = \frac{0.079}{R_{e_L}{}^{0.25}}, C_{f_g} = \frac{0.079}{R_{e_g}{}^{0.25}},$$ $$R_{e_L} = \frac{G_t(1-x)d_i}{u_L}, R_{e_g} = \frac{G_t x d_i}{u_g}, \text{for lamenar flow } C_{f_L} = \frac{16}{R_{e_L}}, C_{f_g} = \frac{16}{R_{e_g}}$$ $$\Phi_L{}^2 = 1 + \frac{C}{x_{tt}} + \frac{1}{x_{tt}{}^2} \text{ for } R_{e_L} > 4000$$

	$$\Phi_g{}^2 = 1 + Cx_{tt} + x_{tt}{}^2 \text{ for } R_{e_L} < 4000$$ $$x_{tt} = \left(\frac{1-x}{x}\right)^{0.9}\left(\frac{\rho_g}{\rho_L}\right)^{0.5}\left(\frac{u_L}{u_g}\right)^{0.1} ,,,, C = 20 \text{ since both flow turbulent}$$
Chisholm's [34]	$$\Phi_{ch}{}^2 = \frac{\Delta P_t}{\Delta P_{Lo}} \text{ or } \Phi_{ch}{}^2 = \frac{\Delta P_t}{\Delta P_{go}} \text{ this reserh used first}$$ $$\Delta P_{Lo} = 4C_{f_{Lo}}\left(\frac{\Delta L}{d_i}\right)G_t{}^2\left(\frac{1}{2\rho_L}\right),, \Delta P_{go} = 4C_{f_{go}}\left(\frac{\Delta L}{d_i}\right)G_t{}^2\left(\frac{1}{2\rho_g}\right)$$ $$C_{f_{Lo}} = \frac{0.079}{R_{e_{Lo}}{}^{0.25}}, C_{f_{go}} = \frac{0.079}{R_{e_{go}}{}^{0.25}}, R_{e_{Lo}} = \frac{G_t d_i}{u_L}, R_{e_{go}} = \frac{G_t d_i}{u_g}$$ $$\text{for lamenar flow } C_{f_{Lo}} = \frac{16}{R_{e_{Lo}}}, C_{f_{go}} = \frac{16}{R_{e_{go}}}$$ $$\Phi_{ch}{}^2 = 1 + (Y^2 - 1)\left(\left(B\left(x^{\frac{2-n}{n}}\right)\left((1-x)^{\frac{2-n}{2}}\right)\right) + x^{2-n}\right), Y^2 = \frac{\Delta P_{go}}{\Delta P_{Lo}}$$ $$\text{for } 0 < Y < 9.5:$$ $$B = \frac{55}{G_t{}^{0.5}} \text{ for } G_t \geq 1900 \frac{kg}{m^2 s}, B = \frac{2400}{G_t} \text{ for } 500 \geq G_t \leq 1900 \frac{kg}{m^2 s}$$ $$B = 4.8 \text{ for } G_t \leq 500 \frac{kg}{m^2 s}$$ $$\text{for } 9.5 < Y < 28:$$ $$B = \frac{550}{YG_t{}^{0.5}} \text{ for } G_t \leq 600 \frac{kg}{m^2 s}, B = \frac{21}{Y} \text{ for } 500 \geq G_t > 600 \frac{kg}{m^2 s}$$ $$\text{for } Y > 28: \quad B = \frac{1500}{Y^2 G_t{}^{0.5}},$$ $$n = 0.25 \text{ used in this study}$$
Friedel [35]	$$\Phi_{Fri}{}^2 = \frac{\Delta P_t}{\Delta P_{Lo}}, \Phi_{Fri}{}^2 = A + \frac{3.24BC}{Fr_H{}^{0.045}We_H{}^{0.035}}, A = (1-x)^2 + x^2\frac{C_{f_{go}}\rho_L}{C_{f_{Lo}}\rho_g},$$ $$B = (1-x)^{0.224} + x^{0.78}, C = \left(\frac{\rho_L}{\rho_g}\right)^{0.91}\left(\frac{u_g}{u_L}\right)^{0.19}\left(1 - \frac{u_g}{u_L}\right)^{0.7}, Fr_H = \frac{G_t{}^2}{gd_i\rho_H}$$ $$We_H = \frac{G_t{}^2 d_i}{\sigma\rho_H}, \rho_{H=}\left(\frac{x}{\rho_g} + \frac{1-x}{\rho_L}\right)^{-1}$$
Muller Steinhagen and Heck	$$\Delta P_t = \left(\Delta P_{Lo} + 2\left(\Delta P_{Lo} - \Delta P_{go}\right)x\right)(1-x)^{\frac{1}{3}} + \Delta P_{go} x^3$$

[36]	
Benbella A. Shannak [37]	$$\Delta P_t = f_{(2ph)}\left(\frac{G_t{}^2 l}{d_i 2\rho_H}\right), \rho_H = \left(\frac{x}{\rho_g} + \frac{1-x}{\rho_L}\right)^{-1},$$ $$R_{e_t} = \frac{G_t d_i\left(x^2 + (1-x)^2\left(\frac{\rho_g}{\rho_L}\right)\right)}{u_g x + u_L(1-x)\left(\frac{\rho_g}{\rho_L}\right)}, f_{(2ph)} = \frac{64}{R_{e_t}} \text{ if } R_{e_t} < 11 \text{ else}$$ $$\frac{1}{\sqrt{f_{(2ph)}}} = -2\log\left(\frac{1}{3.7065}\frac{\varepsilon}{d_i}\right.$$ $$\left. -\frac{5.0452}{R_{e_t}}\log\left(\frac{1}{2.8257}\left(\frac{\varepsilon}{d_i}\right)^{1.1098} + \frac{5.8506}{R_{e_t}{}^{0.8981}}\right)\right)$$
Theissing [38]	$$\Delta P_t = \left(\Delta P_{Lo}^{\frac{1}{n\varphi}}(1-x)^{\frac{1}{\varphi}} + \Delta P_{go}^{\frac{1}{n\varphi}}(x)^{\frac{1}{\varphi}}\right)^{n\varphi}, \varphi = 3 - 2\left(\frac{2\sqrt{\left(\frac{\rho_L}{\rho_g}\right)}}{1 + \left(\frac{\rho_L}{\rho_g}\right)}\right)^{\frac{0.7}{n}},$$ $$n = \frac{n_1 + n_2\left(\frac{\Delta P_g}{\Delta P_L}\right)^{0.1}}{1 + \left(\frac{\Delta P_g}{\Delta P_L}\right)^{0.1}}, n_1 = \frac{\ln\left(\frac{\Delta P_L}{\Delta P_{Lo}}\right)}{\ln(1-x)}, n_1 = \frac{\ln\left(\frac{\Delta P_g}{\Delta P_{go}}\right)}{\ln(x)}$$

Table 3: Two phase flow multiplier equations for bend section

Author or methods	All required equations
A. Azzi, [23]	$$\Phi_L = \frac{\Delta P_t}{\Delta P_L}, Fr_L = \frac{G_t{}^2(1-x^2)}{g d_i \rho_L{}^2}, \Delta P_L = K_L\frac{G_L{}^2}{2\rho_L}, G_L = \frac{m_L}{A}, G_g = \frac{m_g}{A}, G_t = G_L + G_g$$ $$\Phi_L = A + 7.42 Fr_L{}^{0.125}\left(\frac{R}{d_i}\right)^{0.502} x^{0.7}(1-x)^{0.1}\left(\frac{(\rho_L - \rho_g)}{\rho_L}\right)^{0.14}\left(\frac{(u_L - u_g)}{u_L}\right)^{0.12}$$

	$A = (1 - x) + \left(\dfrac{\rho_L\, K_g}{\rho_g K_L}\right) x^2, K_g = f_g \dfrac{L_{eq}}{d_i}, K_L = f_L \dfrac{L_{eq}}{d_i}, f_i = f_g or f_{L,}\ R_i$ $= R_g or R_{L,}$ $f_i = 8\left(\left(\dfrac{8}{R_i}\right)^{12} + \left(\dfrac{1}{(B+C)^{\frac{3}{2}}}\right)\right)^{\frac{1}{12}}, B$ $= \left(2.475 \ln\left(\dfrac{1}{\left(\dfrac{7}{R_i}\right)^{0.9} + \left(0.27\dfrac{\varepsilon}{d_i}\right)}\right)\right)^{16}$ $c = \left(\dfrac{37530}{R_i}\right)^{16}, R_i = \dfrac{G_i d_i}{u_i}$
Chisholm's [39]	$\Phi_L = \dfrac{\Delta P_t}{\Delta P_L}, \Delta P_L = K_L \dfrac{G_L{}^2}{2\rho_L}, B = 1 + \dfrac{2.2}{K_L\left(2 + \dfrac{R}{d_i}\right)}$ $\Phi_L = \dfrac{1}{(1-x)^2}\left(1 + \left(\left(\dfrac{\rho_L}{\rho_g}\right) - 1\right)(Bx(1-x) + x^2)\right)$
Sookprasong [40]	$\Phi_L = \dfrac{\Delta P_t}{\Delta P_L}, \Delta P_L = K_L \dfrac{G_L{}^2}{2\rho_L}, \Phi_L = \dfrac{\left((\rho_L j_L + \rho_g j_g)(j_L + j_g)\right)}{\rho_L\, j_L{}^2}$

ARTICLE

تأثير التدرج الحراري لجريان مائعين (الهواء والماء) على انخفاض الضغط في الانبوب المنحني

لاوان عبدالله فاضل

قسم هندسة الميكانيكية والميكاترونكس، كلية الهندسة، جامعة صلاح الدين – أربيل

lawanabdullahfadhillahmad@gmail.com

عائد عكاب مرعى

قسم هندسة الطيران، كلية الهندسة، جامعة صلاح الدين، أربيل

Iyd.maree@su.edu.krd

الخلاصة

يتضمن هذا البحث دراسة تجريبية لتأثير درجة الحرارة لجريان مائعين (الهواء والماء) على الضغط خلال انبوب (ذو أنحناء (90، على جانبي المنحنى و في المنحنى نفسه. أن هذه الدراسة ذات أهمية لفهم وتحسين العمليات الصناعية التي تنطوي على جريان مائعين. أن التجربة الحالية تتألف من ثلاث اجزاء: أفقي, عمودي, والمسار المنحنى للجريان خلال انبوب مصنوع من مادة (البولي فينيل كلوريد) ويبلغ قطره الداخلي 68 مم ؛ وأما القسم المنحني من الأنبوب يحتوي على نسبة انحناء نصف القطر الى القطر بمقدار 8. (R/D) وقد تم أستخدام مجموعة متنوعة من معدلات تدفق المياه التي تراوحت من 18 إلى 42 متر مكعب في الساعة وأما معدلات جريان الهواء فقد تراوحت بين 4 إلى 18 متر مكعب في درجات الحرارة مختلفة ، وقد تم استخدام ستة مجسات ضغط لمراقبة الضغط خلال مدة التجربة . وقد تمت مقارنة النتائج التجريبية لهبوط الضغط التي تم الحصول عليها من التجربة ومقارنتها مع النماذج المنشورة مسبقًا لتقييم نتائج أدائها في التنبؤ بانخفاض الضغط في ظروف انتقال الحرارة ولكن بدون الغليان .بناءً على النتيجة التجريبية ، يزداد الضغط عبر أجزاء التجربة مع زيادة درجة حرارة في الحالة التي لا تهيمن فيها لزوجة السائل على لزوجة الخليط نظرًا لارتفاع معدل تدفق السائل أيضًا ، يكون انخفاض الضغط عبر المنحنى عالياً عندما يكون معدل تدفق الهواء قليلاً مقارنة بمعدل تدفق هواء ألعالي عند ثبوت معدل تدفق الماء و عند درجة حرارة الغرفة ، و تنعكس الحالة بزيادة درجة حرارة الخليط حيث أن أنخفاض الضغط عند معدل تدفق الهواء العالي . تكون أعلى بالمقارنة مع معدل تدفق الهواء المنخفض. وكشفت الدراسة بان الحرارة تزيد الضغط و هبوط الضغط عند المنحنى لجريان مائعين عند معدلات تدفق الهواء العالية بثبوت معدل جريان الماء .

الكلمات الدالة : انخفاض الضغط ، جريان الطورين (الهواء والماء)، انبوب منحنى 90، تاثير درجة الحرارة.